Lasers in Manufacturing Conference 2021

Laser machining of different steel grades with 10ps laser pulses: The influence of carbides onto the surface roughness and structures for different laser parameters

S. M. Remund[a*], S. N. Herren[a], J. Zuercher[a], A. Kipka[a], B. Neuenschwander[a]

[a]*Bern University of Applied Sciences, Institute for Applied Laser, Photonics and Surface Technologies, Pestalozzistrasse 20, 3400 Burgdorf, Switzerland*

Abstract

When steel is machined with ultra-short pulses the specific removal rate strongly depends on the pulse fluence, the wavelength and, in case of bursts, on the number of pulses whereas the steel grade has a minor influence. This situation changes for the surface roughness. Beside the laser parameters, the initial surface, and the number of machined layers the obtainable surface roughness also depends on the carbides located in the steel as well as their size and distribution and therefore it is strongly influenced by the steel grade. E.g. for a given set of parameters a surface roughness S_a value of 0.18 µm, 0.25 µm and 0.39 µm was achieved for CK75 (no carbides), M390 (small carbides) and K100 (large carbides). We present the results of a systematic study for different steel grades in the application of surface structuring and smoothening of surfaces machined by alternative technologies as e.g. electrical discharge machining (EDM).

Keywords: ultra-short pulses; steel; surface roughness; influence of carbides;

1. Introduction

Steels with carbides in a martensitic microstructure are hard and feature a high wear resistance. Therefore, such steels are often used to produce high performance tools as e.g. molds, cutting- and stamping tools depending on their composition and microstructure. To ensure the demanded precision of the tool, the finishing processes are often made in the final hardened condition. Using conventional machining strategies on hard materials is challenging and expensive due to attrition of the tools. Hence technologies like electrical

* Corresponding author. Tel.: +41 34 426 42 21
E-mail address: stefan.remund@bfh.ch

discharge machining (EDM) or laser machining are often used. In EDM the material removal is based on electrical energy, which generates a plasma channel between the workpiece and the tool-electrode as described by Ho et al. at temperature ranges between 8'000 and 12'000 °C or even as high as 20'000 °C, so the workpiece material at this point melts and vaporizes. However, a part of the molten material resolidifies on the workpiece and form a brittle layer with altered microstructures and mechanical properties often called heat affected zone (HAZ). For most applications this layer needs to be removed requiring an additional processing step. Ultra-short pulse lasers (USP) are known for material removal with a minimal HAZ and are already reported as an alternative material processing technology to EDM e.g. in the paper of Dumitru et al. Furthermore, USP ablation can be used to remove this brittle layer and offering the possibility of surface structuring in the micrometer scale and thus an additional surface functionalization in one processing step.

2. Experimental Setup and methods

For the comparison of different wavelengths two laser systems are used. The laser system PicoBlade2 from Lumentum is used for the experiments in the near-infrared, supplying pulses with 10 ps pulse duration at 1064 nm wavelength. The experiments with 532 nm wavelength and 10 ps pulse duration are made with the laser system Fuego from Lumentum (former Time-Bandwidth), which provides an internal SHG for wavelength conversion. The beam lines of both systems are similar organized: The average laser power P_{av} on the sample can be controlled by a motorized λ/2 plate and a thin-film polarizer. The beam paths are guided by several folding mirrors trough a beam expander onto a galvanometer scanner and a λ/4 and a λ/2 plate are introduced and aligned to achieve circular polarization on the sample. For the 1064 nm beam line, the galvanometer scanner excelliSCAN14 from Scanlab with a mounted telecentric 100 mm focal length objective is used, reaching a waist radius of $w_{0,1064nm}$ = 11 µm with a $M^2_{1064nm} \leq 1.5$. In the 532 nm setup an intelliSCAN$_{se}$14 scanner from Scanlab with mounted telecentric 100 mm focal length objective is used, reaching a $w_{0,532nm}$ = 4.7 µm with a $M^2_{532nm} \leq 1.13$ on the sample. The scanners are controlled by our synchronization electronic named Synchro V3.0, which enables a repeatable laser pulse positioning on the sample with sub-micrometer accuracy at full scan speed. A detailed description of the Synchro V3.0 technology can be found in the papers from Jaeggi et al. and Gafner et al. To study the material behavior for surface structuring, 2.5-D shaping and milling applications, squares with a side length of around s = 1 mm are machined. The pulse to pulse and the line distance is set to $p_{x,1064nm} = p_{x,1064nm}$ = 5.5 µm and $p_{x,532nm} = p_{x,532nm}$ = 2.1 µm and the squares are scanned by only straight lines without hatching angle. For all experiments a laser pulse repetition frequency f_{rep} = 2 MHz is set.

Both laser systems support a pulse burst operation, whereby instead of just a single pulse per repetition frequency cycle, a certain number of pulses with a close separation of 12.2 ns is emitted. Additionally, the implemented FlexBurst™ technology features the possibility to individually adjust the energy of every pulse in the burst. This is used to adapt the energy of each pulse in the burst to equal height i.e. equal pulse energy for all experiments with pulse bursts in this work. The following pulse burst variations are used: single pulse (1PB), two pulses per burst (2PB), three pulses per burst (3PB) and four pulses per burst (4PB). As discussed by Neuenschwander et al. if pulse bursts are used to compare their performance, the average power must be divided by the number of pulses per burst n_b for the laser peak fluence calculation and hence the peak fluence of each single pulse in the burst is given by equation (1):

$$\phi_0 = \frac{2 \cdot P_{av}}{f_{rep} \cdot \pi \cdot w_0^2 \cdot n_b} \tag{1}$$

Furthermore, the number of ablation layers n_r is divided by the number of burst pulses n_b to apply the same number of pulses per area. If not otherwise mentioned for a 1PB operation n_r is set to 192 and as an

example for a 3PB n_r is set to 64. After machining, the ablation depth d is measured with a white light interferometric microscope smartWLI from GBS combined with the image analysis software MountainsMap from Digital Surf. With this measurement the specific ablation rates γ_{spec} given by the following equation (2) are calculated.

$$\gamma_{spec} = \frac{p_x \cdot p_y \cdot d \cdot f_{rep}}{n_b \cdot n_r \cdot P_{av}} \tag{2}$$

The point where the specific removal rate reaches its maximum value is called optimal point and the corresponding peak fluence optimal fluence. At this point the ration between inserted energy and introduced material ablation is at its maxima.

As an measure of the machining quality the surface roughness value S_a is analyzed, which is calculated for the surfaces in MoutainsMap according to ISO 25178. Supplementary, some structures are imaged by the scanning electron microscope (SEM) Sigma VP from Zeiss to get an impression of the structure sizes and for comparison of the parameters.

If not otherwise mentioned the experiments are made on initially polished sample surfaces.

3. Examined Materials

To study the behavior of carbides, their size and the steels microstructure when machined with ultra-short laser pulses, the three different steel grades M390, K100 and CK75 are examined in this work. Fig. 1. Illustrates the microstructure of these three steels in hardened condition.

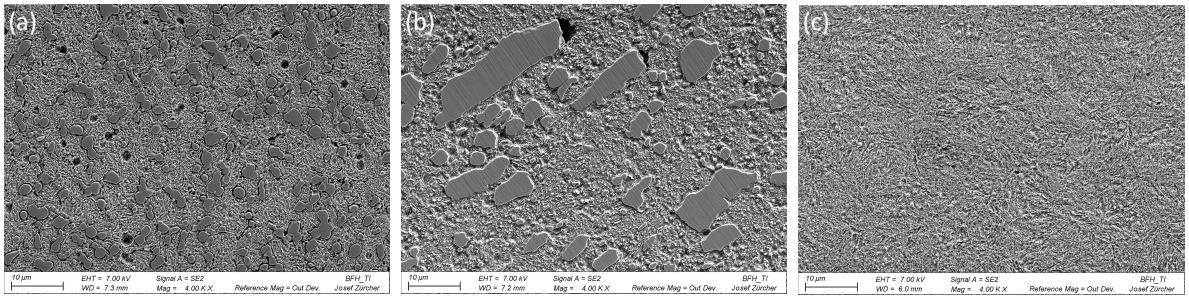

Fig. 1. Microstructure of the studied steel grades visualized by etching and imaged by SEM. (a) M390 in hardened condition with approx. 3 µm carbides in a martensitic matrix, (b) K100 in hardened condition with bigger carbides up to tens of micrometer in a martensitic matrix and (c) CK75 in hardened condition with a martensitic microstructure without carbides.

M390 from Böhler is a powder metallurgical produced steel often used for plastic molds and cutting tools. The high content of carbon and chromium as listed in Table 1. and the alloying elements molybdenum, vanadium and tungsten lead to formation of hard carbides. M390 is examined in hardened and tempered condition. This heat treatment results in a martensitic microstructure with embedded carbides. Our material reached a hardness of 825 HV10.

K100 from Böhler is a dimensionally stable, ledeburitic tool steel with high content of carbon and chromium as listed in Table 1. The formation of chromium carbides directly from the melt pool effects their dimension and leads to carbide sizes up to tens of micrometer. In hardened and tempered condition with a martensitic microstructure around the carbides our material reached a hardness of 699 HV10.

CK75 from Notz Metall with the brand name NOTZ 70 blau is an unalloyed spring steel. The material is supplied with pretreatment cold rolling, hardening and tempering. The martensitic microstructure induces a hardness of 487 HV10.

The given hardness for each material is an average of five Vickers tests.

Table 1. Chemical composition in average mass percent of the studied steel grades. Iron (Fe) is added in balance to 100%.

Name	C	Si	Mn	Cr	Mo	V	W	P	S
M390	1.90	0.70	0.30	20.00	1.00	4.00	0.60	-	-
K100	2.00	0.25	0.35	11.50	-	-	-	-	-
CK75	0.70 - 0.95	0.15 - 0.30	0.50 - 0.80	-	-	-	-	max. 0.03	max. 0.02

4. Experimental Results

In this section, the Results of three separate studies are presented. The influence of the laser parameters onto the ablation behavior and the resulting surface roughness on M390 is initially shown. Furthermore, ablation results on three different steel types K100 with large carbides, M390 with small carbides and CK75 without carbides are compared. The last subsection discusses the application of USP processing for smoothening of surfaces, resulting from wire-cut EDM on M390.

4.1. Ablation behavior of M390 different sets of laser parameters

Ablations studies on M390 with different set of laser parameters are shown in Fig. 2. The highest specific removal rate is reached with single pulses (1PB) at 532 nm, which is slightly higher than the rate reached with single pulses at 1064 nm. A decreasing ablation efficiency is indicated for the laser parameters with pulse bursts. Specially the experiments at 1064 nm with increasing number of pulses per burst shows this sequential decrease. However, the curves with the 3PB and 4PB reveal similar ablation rates and therefore, at least a temporary saturation of this reduction. A similar trend is described by Neuenschwander et al. on the steel AISI 304 (1.4301). The 3PB with both examined wavelengths reaches similar maximum specific removal rates, which are slightly over 20% less efficient to their corresponding rates with single pulses. So, the ablation depth reached with 3PB for a certain number of layers is 20% smaller than the depth reached with single pulses and three times the layer count, since the comparison is based on the same applied pulses per area.

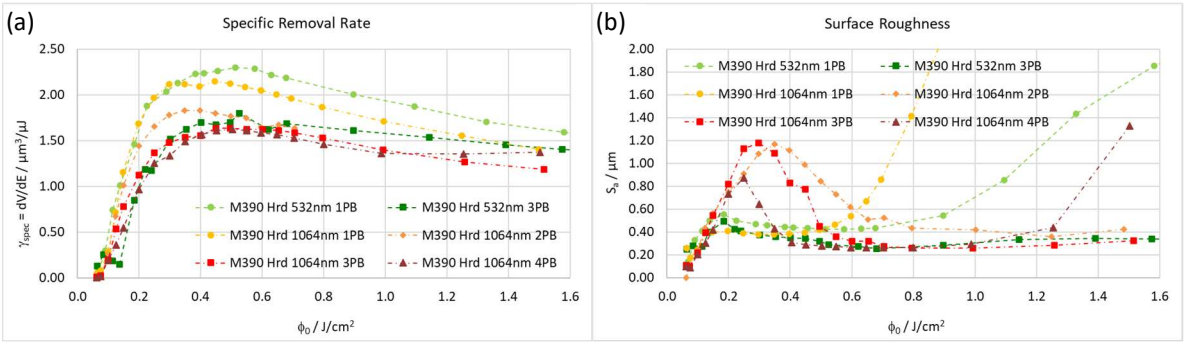

Fig. 2. Experimental results on M390 with different laser parameters. (a) showing the specific removal rates with 532 nm and 1064 nm for single pulses and pulse bursts and (b) the corresponding surface roughness.

With all examined laser parameters, a minimal surface roughness S_a beneath 0.40 µm is reached except for the single pulse operation at 532 nm, which is just slightly above, indicated in Fig. 2. (b). However, the peak fluences, where these minima are reached differ and at 1064 nm with pulse bursts an initial increase of the roughness for low fluences is observed, which reclines for increasing fluences. Higher roughness values indicate the formation of cavities or in literature often called cone like protrusions (CLP) as discussed by Bonse et al. Since, usually the cavity formation appears at higher fluences, specially the behavior with the 2PB is surprising, where the maximum roughness is reached at a peak fluence of around 0.4 J/cm^2, which is close to the optimal point, where the specific removal rate is at its maxima. The smallest surface roughness with about 0.26 µm are reached with the 3PB at 532 nm and the 3PB and 4PB at 1064 nm.

4.2. Comparison of M390, K100 and CK75 concerning specific ablation rate and surface roughness

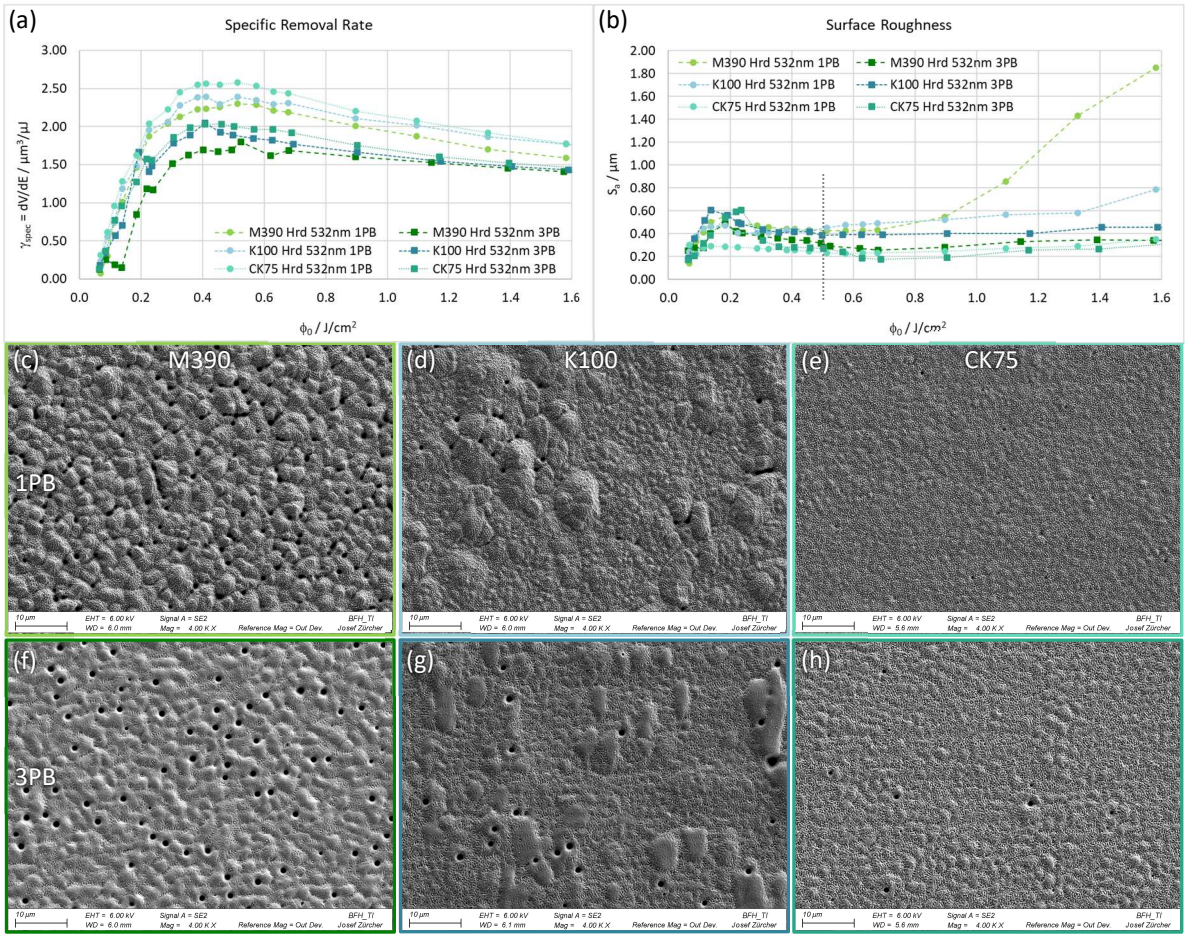

Fig. 3. Experimental results on M390, K100 and CK75 in hardened (Hrd) condition at 532 nm for different peak fluences and pulses per burst. (a) is showing the specific removal rates and (b) the corresponding reached surface roughness. The SEM images represents the surface after ablation with a peak fluences of 0.5 J/cm2 and a 1PB of (c) M390, (d) K100 and (e) CK75 and with the same single pulse fluence and a 3PB of (f) M390, (g) K100 and (h) CK75.

The specific removal rate for the examined steel types in hardened condition differ slightly for the same set of laser parameters at 532 nm as indicated in Fig. 3. (a). Where on CK75 without carbides the highest and on M390 the lowest rates are archived. This difference is less prominent at 1064 nm, but with the same trend as shown in Fig. 4 (a). At both wavelengths the ablation with 3PB is around 20 to 25% less efficient for all three steel types. The resulting surface roughness with 532 nm plotted in Fig. 3. (b) are generally low and mainly only increase for K100 and M390 at higher fluences with single pulses. At 1064 nm with single pulses a similar behavior but with a faster increase of the roughness at higher fluences is observed as shown in Fig. 4. (b). As mentioned in the previous section this increase is often cause by the formation of cavities, which is also shown in Fig. 4. (c). This point of cavity formation seams to shift if higher average power is used, as with the 3PB at 1064 nm an increased roughness at lower fluences appears on all three steel types.

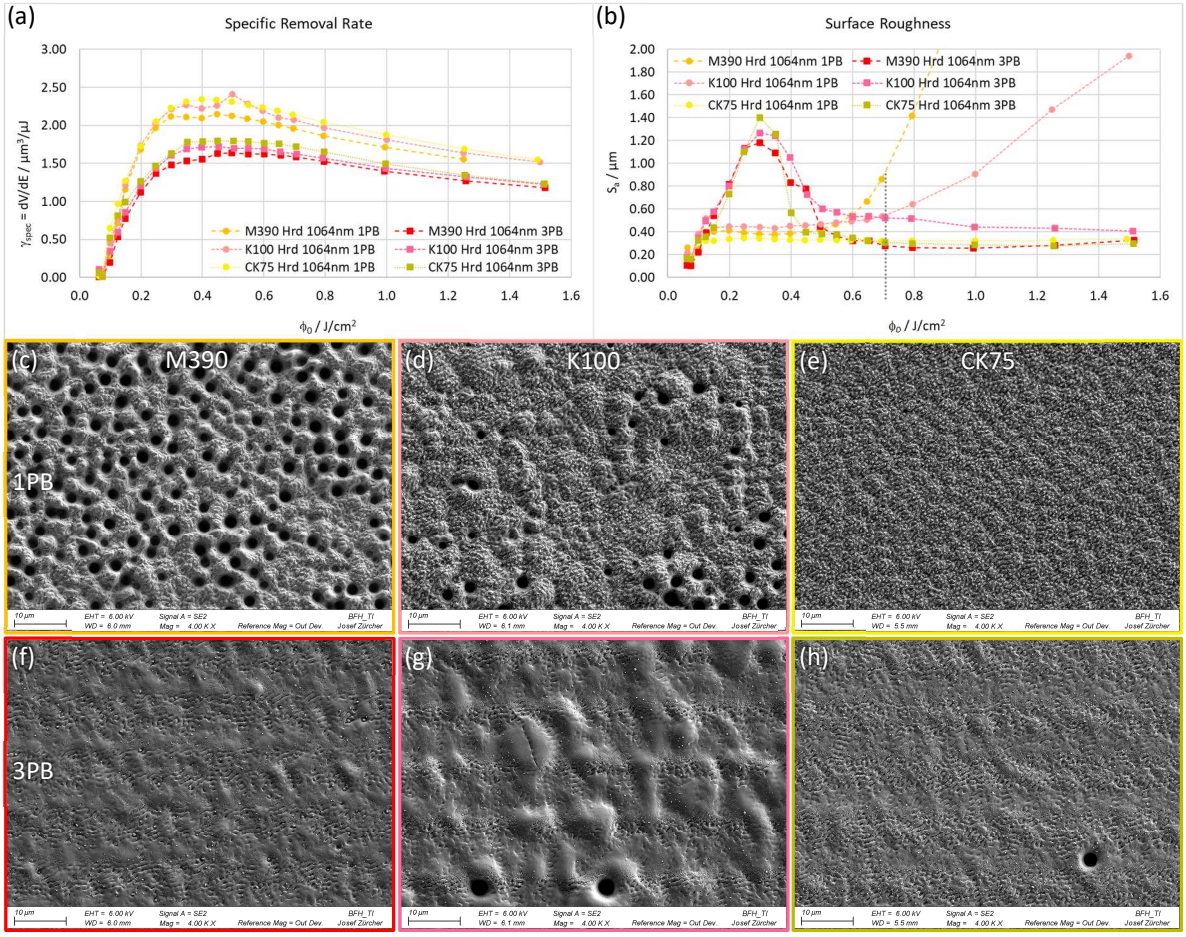

Fig. 4. Experimental results on M390, K100 and CK75 in hardened (Hrd) condition with 1064 nm for different peak fluences and pulses per burst. (a) is showing the specific removal rates and (b) the corresponding surface roughness. The SEM images represents the surface after ablation with a peak fluences of 0.7 J/cm² and a 1PB of (c) M390, (d) K100 and (e) CK75 and with the same single pulse fluence and a 3PB of (f) M390, (g) K100 and (h) CK75.

The acquired surfaces of CK75 Fig. 3. (e), (h) and Fig. 4. (e), (h) present a homogenous ablation and a resulting smooth surface, thus similar smooth surfaces are reached on this material with all examined laser parameters. The images of K100 processed with 3PB illustrated in Fig. 3. (g) and Fig. 4. (g) for both wavelengths indicate protrude structures with shape and size in order of the carbides shown in Fig. 1. (a). An energy-dispersive X-ray (EDX) analysis on these surfaces confirms this impression. In Fig. 3. (d) showing K100 processed with single pulses at 532 nm the carbides are indicated as well but less pronounced. Thus, the higher roughness values on K100 is caused by the carbides exhibiting a different ablation behavior. Corresponding to this, structures of the smaller carbides are sightly visible on the image of M390 machined with 3PB in Fig. 3. (f) and Fig. 4. (f). Furthermore, M390 machined with 1PB and 0.7 J/cm^2 at 1064 nm already leads to the discussed cavity formation which are visualized in Fig. 4. (c).

The smallest roughness is reached on all three materials with a 3PB at 532 nm with the values 0.18 µm for CK75, 0.25 µm for M390 and 0.39 µm for K100.

4.3. Smoothening of EDM surfaces on M390

For this experiment a M390 plate in hardened condition was cut by wire-cut EDM with stage wise different parameters resulting in five surface sections with increasing roughness values of $S_{a,init1}$ = 0.53 µm, $S_{a,init2}$ = 0.68 µm, $S_{a,init3}$ = 1.34 µm, $S_{a,init4}$ = 1.85 µm and $S_{a,init5}$ = 3.26 µm. On these surfaces the application of roughness smoothening is investigated, which potentially could be combined with a surface functionalization by simultaneously introducing certain structures. Due to the experiments in the preceding results, for this application a 3PB with a peak fluence of 0.7 J/cm^2 of each single pulse at both wavelengths are chosen as laser parameters. The graphs on top of Fig. 5 represent the relative smoothing, so the measured surface roughness S_a after a given number of layers in relation to the specific initial surface roughness $S_{a,init}$. Below the initial structures of three of these surfaces, surface 1, 3 and 5 and the results after 8 and 128 layers on them are shown. Each experiment for a specific number of layers is made on a sperate position and not sequentially on the same position of the sample. This and the appearance of cracks in EDM processed surfaces, which may appear in different counts in the field of measurement, cause the variance of the datapoints, specially at surfaces with higher initial roughness values. The plotted results indicate that a smoothening of all surfaces is reached with the chosen laser parameters at both wavelengths. The study at 532 nm on surface 1 with the lowest initial roughness of $S_{a,init1}$ = 0.53 µm shown in Fig. 5. (c) pose an optimal number of layers for smoothening. With 24 layers a roughness of S_a = 0.33 µm is reached but increases for increasing number of layers. This is caused by the growing appearance of cavities as illustrated in the SEM images taken for 8 layers ablation on Fig. 5. (f) and 128 layers ablation on Fig. 5. (i). At 1064 nm and the chosen laser parameters the cavity formation is much less pronounced, which is indicated by the steadily trend of the roughness values in Fig. 5. (a) at lower roughness values. Specially for surface 1 and 2 the achievable smoothening is reached already after 8 to 24 layers and stays constant for increasing number of layers at 1064 nm. The performance on surface 3 with a initial roughness of $S_{a,init3}$ = 1.34 µm is similar for both wavelengths and a nearly linear decrease of the roughness over increasing layer numbers is shown. For surface 4 and 5 with a higher initial roughness the smoothening with the laser parameters at 532 nm is more distinct with a linear tend in average as well. However, the high variance of the measured points leaves a small uncertainty and therefore, a study with more datapoint should be conducted to support this implication. On Fig. 5. (e) the surface 5 with jagged structures is visualized causing its high roughness value of $S_{a,init5}$ = 3.26 µm. Even after 128 layers and an ablation depth of approximately 34 µm cracks are still visible and not fully removed as shown in Fig. 5. (k) for the laser parameters at 532 nm.

By comparing the final surfaces reached, a diameter difference of the formed cavities at 532 nm in Fig. 5. (i) and (k) to the ones formed at 1064 nm (j) is noticeable, where the ones formed at 523 nm are around half the

size. However, a direct relation to the used wavelength is not obvious and the nearly six times higher average power used at 1064 nm to reach the same fluence might be the reason for the difference in size. However, further investigations would be necessary to clarify this behavior.

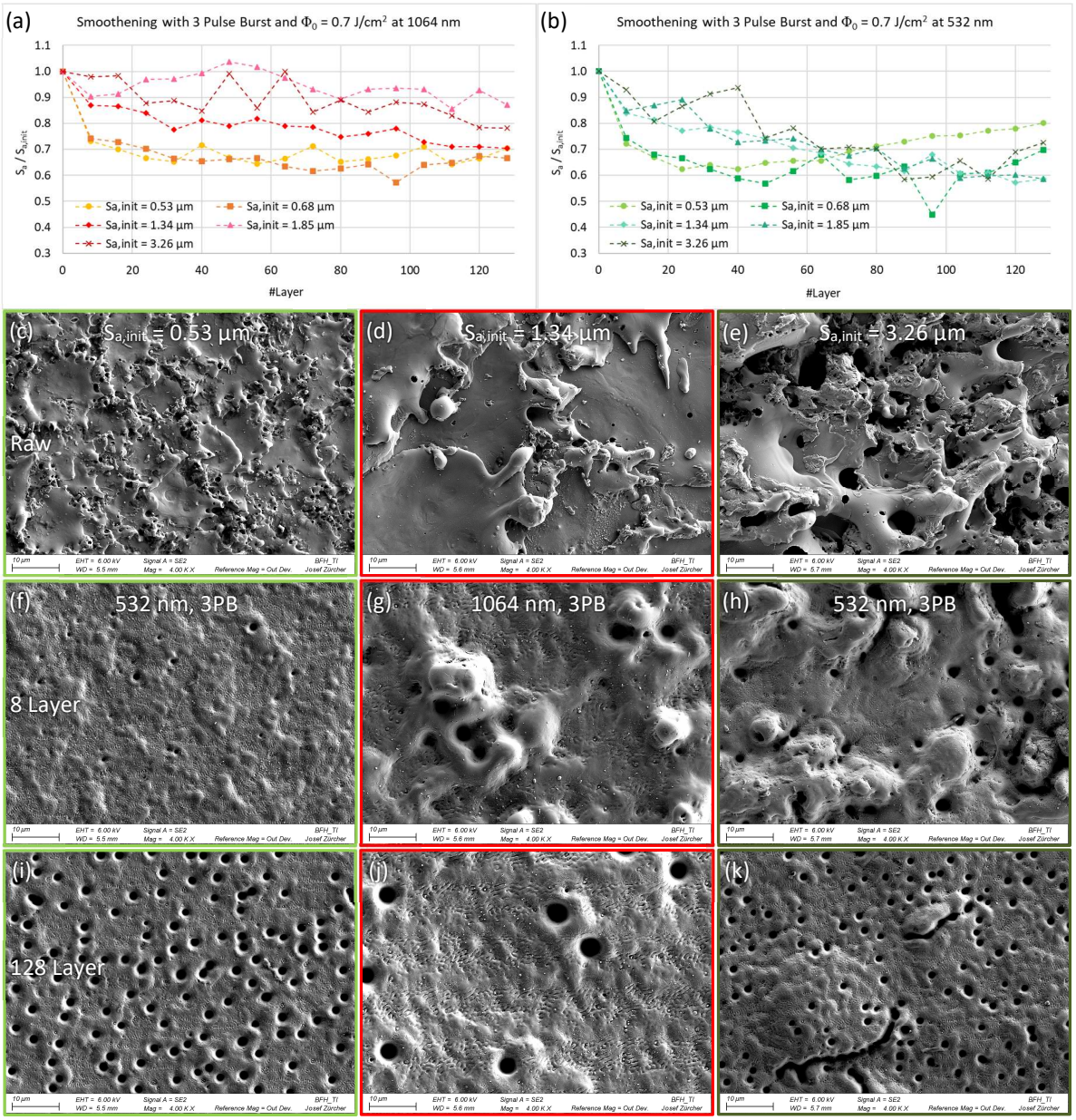

Fig. 5. Results for roughness smoothening trial on initially wire-cut EDM surfaces. The roughness reduction in relation to the initial value is given for a set of laser parameters in (a) for 1064 nm and in (b) for 532 nm wavelength. The structure of three initial surfaces (c), (d) and (e), the result after 8 layers (f), (g) and (h) and the results after 128 layers is shown.

Conclusion

The ablation studies on M390 with different laser parameters at two wavelengths have shown a slightly higher ablation rate for 532 nm as for 1064 nm at single pulses. For the 3PB a decrease of the ablation efficiency of over 20% compared to single pulses was measured for both wavelengths reaching similar ablation rates in this burst operation. The two other examined materials K100 and CK75 behaved similarly, but slightly higher ablation rates were reached, where CK75 achieved the highest and therefore M390 the lowest for all laser parameters at both wavelengths, but within a range of less than 20%. Concerning the resulting surface roughness on the ablated areas, low variations for the experiments at 532 nm were measured on alle materials, except for peak fluences above 0.9 J/cm^2 for single pulse as an increase of the roughness on M390 and K100 with increasing fluence is indicated. At 1064 nm the same increase but beginning already at a peak fluence of 0.7 J/cm^2 and a faster rising was observed for single pulses. However, the behavior with a 3PB at 1064 nm totally changes, where rising the peak fluence to 0.6 J/cm^2 leads first to an increase of the roughness up to 1.3 µm followed by a decline for all three materials. On the SEM images of K100 protrude structures of remaining carbides are visible and regarding to this also on M390 protrude carbides are noticeable but only at 3PB operation. It is assumed, that the carbides have a different ablation behavior as the embedding martensitic matrix, probably at least caused by a different threshold fluence, which induces the remaining carbides. However, further investigations are needed to get a deeper understanding on the influence of carbides. For single pulses on M390 the formation of rougher structures and cavities specially at 1064 nm is visible. In contrary to this CK75 without carbides in the microstructure shows a very smooth and regularly surface at all examined laser parameters except for the mentioned 3PB at 1064 nm with low fluences. The smallest roughness values on all three materials were reached with a 3PB at 532 nm with the values 0.18 µm for CK75, 0.25 µm for M390 and 0.39 µm for K100.

With the 3PB operation it was shown that on all previous EDM threaded surfaces a roughness reduction was achieved. Even on the initially smoothest roughness with $S_{a,init1}$ = 0.53 µm a reduction onto a roughness of S_a = 0.33 µm was demonstrated. However, due to the formation and growing appearance of cavities over increasing number of layers, the surface roughness increases specially with the laser parameters at 532 nm.

It was generally shown, that for lower initial surface roughness values, a maximum smoothening was reached with a relatively low number of ablation layers as between 8 to 24. At 1064 nm the roughness values stayed almost constant for increasing number of layers after its minimum value was obtained. On surfaces with initial roughness values $S_{a,init3}$ = 1.34 µm and $S_{a,init4}$ = 1.85 µm a roughness reduction with a linear decreasing trend was measured. A more successful surface smoothening with the laser parameters at 532 nm for higher initial roughness values was observed.

Acknowledgements

Special thanks to Silvana Schio for organizing the material and here support with the metallurgic preparations and to Markus Gafner for supporting the laser experiments.

References

Böhler K100: Product datasheet, voestalpine BÖHLER Edelstahl GmbH & Co KG, Feb. 2010.

Böhler M390 microclean: Product datasheet, voestalpine BÖHLER Edelstahl GmbH & Co KG, May 2019.

Bonse, J., Höhm, S., Kirner, S. V., Rosenfeld A., and Krüger, J., 2017. ”Laser-Induced Periodic Surface Structures— A Scientific Evergreen,” in IEEE Journal of Selected Topics in Quantum Electronics. Vol. 23, no. 3, Art no. 9000615.

CK75, Notz 70 blau – 1.1248 gehärtet und angelassen, Notz Metall, Dec. 2006.

Dumitru, G., Lüscher, B., Krack, M., Bruneau, S., Hermann, J., Gerbig, Y., 2005. “Laser processing of hardmetals: Physical basics and applications,” International Journal of Refractory Metals and Hard Materials. Volume 23, Issues 4–6.

Gafner, M., Remund, S., Neuenschwander, B., Mähne, T., 2018. ”Optimized Strategies for Galvo Scanning in Fully Synchronized Mode Leading to Massive Improvement in Maching Time,” 37th International Congress on Applications of Lasers & Electro Optics ICALEO. Orlando, Florida, USA, paper M601

Ho, K.H., Newman, S.T., 2003. “State of the art electrical discharge machining (EDM),” International Journal of Machine Tools and Manufacture. Volume 43, Issue 13.

Jaeggi, B., Neuenschwander, B., Hunziker, U., Zuercher, J., Meier, T., Zimmermann, M., Selbmann, K. H., Hennig, G., 2012. “Ultra high precision surface structuring by synchronizing a galvo scanner with an ultra short pulsed laser system in MOPA arran-gement,“ Proceedings of SPIE vol. 8243.

Neuenschwander, B., Kramer, T., Lauer, B., Jäggi, B., 2015. ”Burst mode with ps- and fs-pulses: Influence on the removal rate, surface quality and heat accumulation,” Proc. SPIE 9350, Laser Applications in Microelectronic and Optoelectronic Manufacturing (LAMOM) XX. San Francisco, California, USA, paper 93500U